



Enhancing Turbulence Fluctuation Measurements with Tailored Wind Lidar Profilers

Maxime Thiébaud

Maxime.Thiebaut@france-energies-marines.org



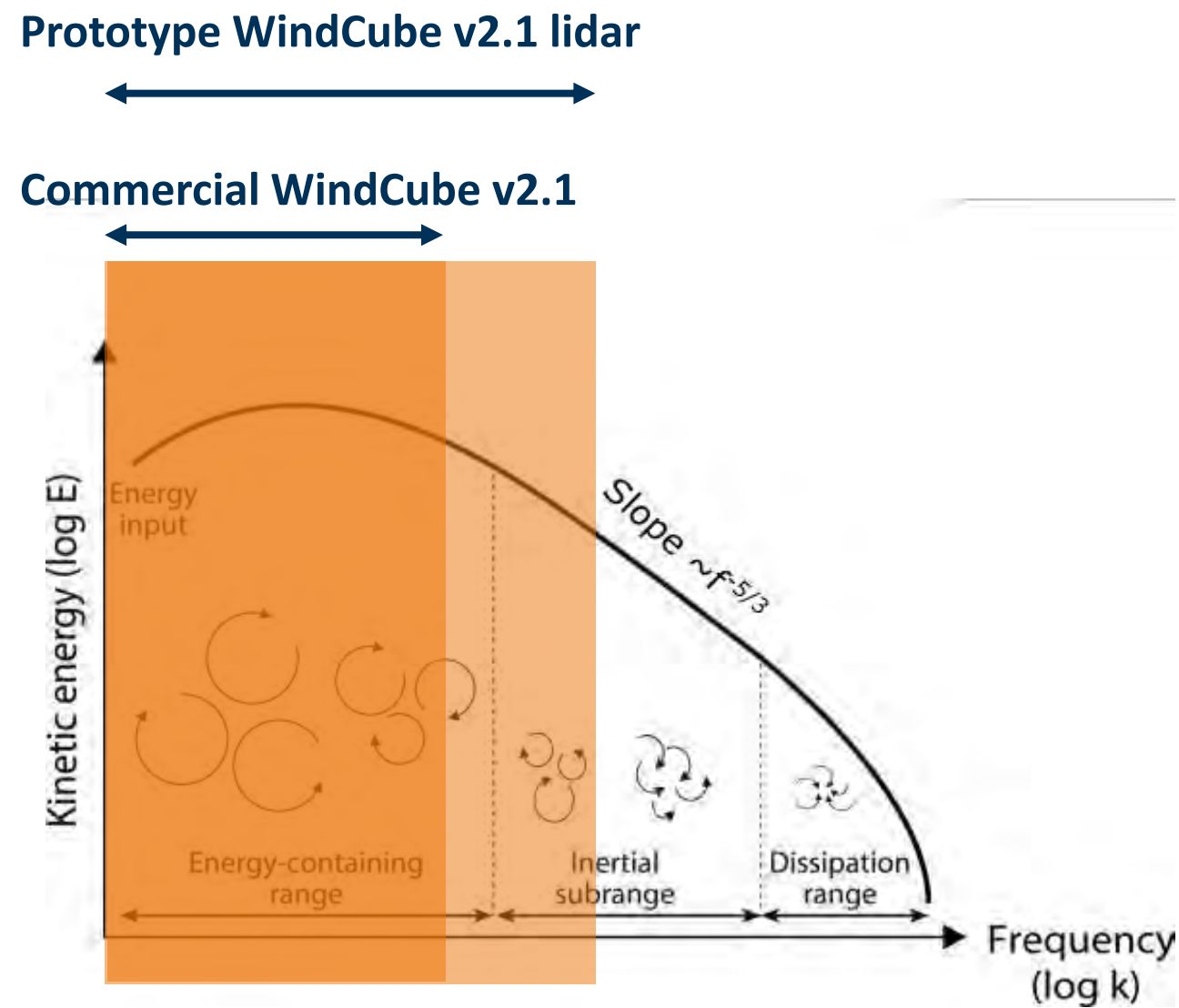
Deployment of wind and turbulence observations in the Mediterranean Sea

1. Enhancing Turbulence Measurement with Tailored Wind Lidar Profilers: Application to WindCube v2.1
2. Optimizing Sparse Sampling for Offshore Wind Resource Assessment in the Mediterranean Sea
3. Deploying a Wind Lidar Profiler on Le Planier Island, Mediterranean Sea
4. Developing a Preliminary Motion-Compensation Algorithm for Floating Lidar Turbulence Measurement

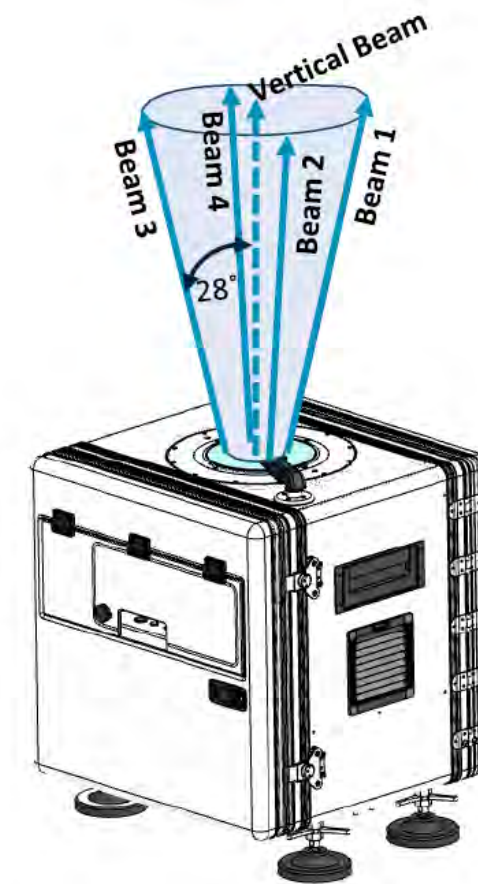
Enhancing Turbulence Measurement with Tailored Wind Lidar Profilers: Application to WindCube v2.1

Increase of the Sampling Rate of Line-of-Sight velocities

Collaboration with Vaisala to build a prototype wind lidar profiler sampling line-of-sight (LOS) velocities 4x faster.



Prototype lidar:
Sampling rate of LOS velocities x4



New version submitted for review this month

Enhancing turbulent fluctuation measurement with tailored wind lidar profilers

Maxime Thiébaud¹, Frédéric Delbos², and Florent Guinot¹

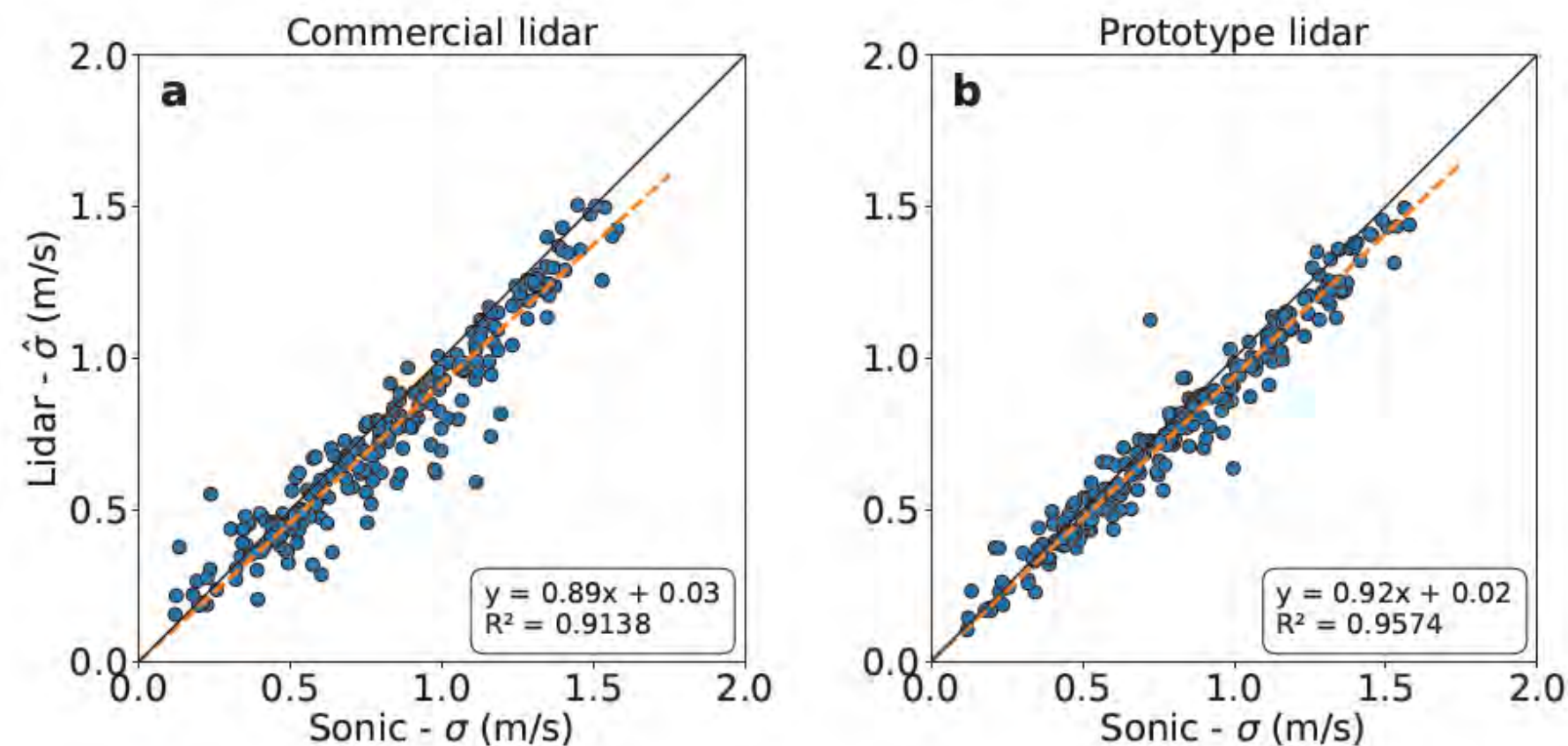
¹France Énergies Marines, Technopôle Brest-Iroise, 525 Avenue Alexis de Rochon, 29280 Plouzané, France

²Vaisala France SAS, 6A, rue René Razel, Tech Park, CS 70001, 91400 Saclay Cedex, France

Correspondence: Maxime Thiébaud (maxime.thiebaud@france-energies-marines.org)

Increase of the Sampling Rate of Line-of-Sight velocities

- **Prototype vs. Commercial Setup:** The prototype WindCube v2.1 lidar showed similar performance to the commercial version for key performance indicators (KPIs) such as slope, coefficient of determination mean wind difference of mean wind speed.
- **Data Availability:** The prototype lidar had **0.5% lower data availability** compared to the commercial configuration.
- **Turbulence Measurement:** The **mean noise-corrected along-wind variance** measured by the prototype was **~7% higher**, suggesting improved capability to capture smaller eddies, especially at higher wind speeds.



Physical Oceanography

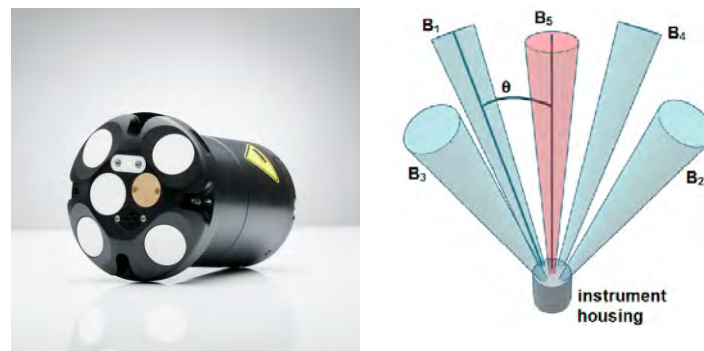
Reynolds Stress and Turbulent Energy Production in a Tidal Channel

TOM P. RIPPETH, EIRWEN WILLIAMS, AND JOHN H. SIMPSON

School of Ocean Sciences, University of Wales Bangor, Menai Bridge, Anglesey, United Kingdom

(Manuscript received 22 March 2001, in final form 7 September 2001)

etermination of Reynolds stress profiles using an ADCP. This method, which relies on comparing velocity variances of opposing beams, is known as the “variance” method and has been employed in a number of shelf and estuarine studies of the evolution of the structure of turbulence (van Haren et al. 1994; Stacey et al. 1999a,b; Lu and Lueck 1999; Lu et al. 2000). The method also provides an estimate of the turbulent kinetic energy (TKE) and of the rate of production of TKE.



5-beam ADCP (acoustic Doppler current profiler)

Atmospheric Science

Doppler Lidar Measurement of Profiles of Turbulence and Momentum Flux

WYNN L. EBERHARD AND RICHARD E. CUPP

NOAA/ERL Wave Propagation Laboratory, Boulder, Colorado

KATHLEEN R. HEALY

CIRES, University of Colorado, Boulder, Colorado

(Manuscript received 14 September 1988, in final form 22 March 1989)

The variance method has been used in Oceanic and Atmospheric science since the late 80s and beginning 90s.

Turbulence intensity (TI) from lidar measurements can be retrieved using two methods: the standard method and the variance method.

- **Standard method**

Computation of the second-order statistics of the three velocity components directly from the reconstructed velocity components, which have been already computed based on the LOS velocities.

TI measurements disturbed by:

1. Inter-beam effect
2. Intra-beam effect
3. Noise
4. Low sampling rate



Increasing the sampling will « feed » the inter-beam effect

- **“Variance” method (developed in POWSEIDOM)**

Computation of second-order statistics of the three velocity components based on the second-order statistics of the LOS velocities.

TI measurements disturbed by:

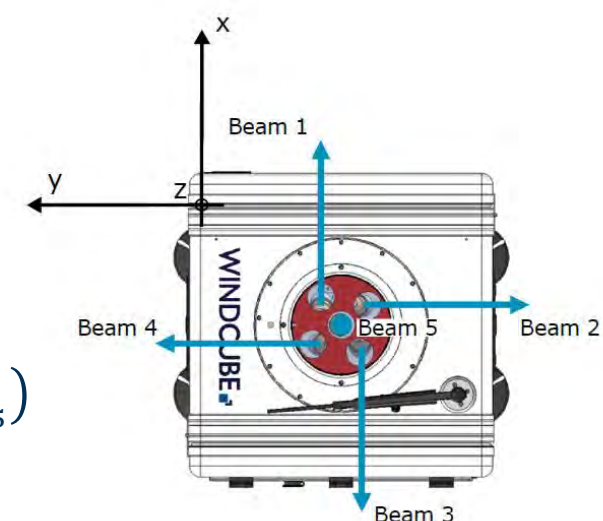
1. Intra-beam effect
2. Noise (can be identified and removed)
3. Low sampling rate

$$\sigma_u^2 = \sigma_x^2 \cos^2 \vartheta + \sigma_y^2 \sin^2 \vartheta + \sigma_{xy} \sin 2\vartheta$$

↖ Wind direction
↙ Unknown

$$\sigma_x^2 = \frac{1}{2\sin^2\theta} (\sigma_{p_3}^2 + \sigma_{p_1}^2 - 2\cos^2\theta\sigma_{p_5}^2) \quad \text{and} \quad \sigma_y^2 = \frac{1}{2\sin^2\theta} (\sigma_{p_2}^2 + \sigma_{p_4}^2 - 2\cos^2\theta\sigma_{p_5}^2)$$

$\sigma_{p_i}^2$: Variance of LOS velocities corrected from instrumental noise.

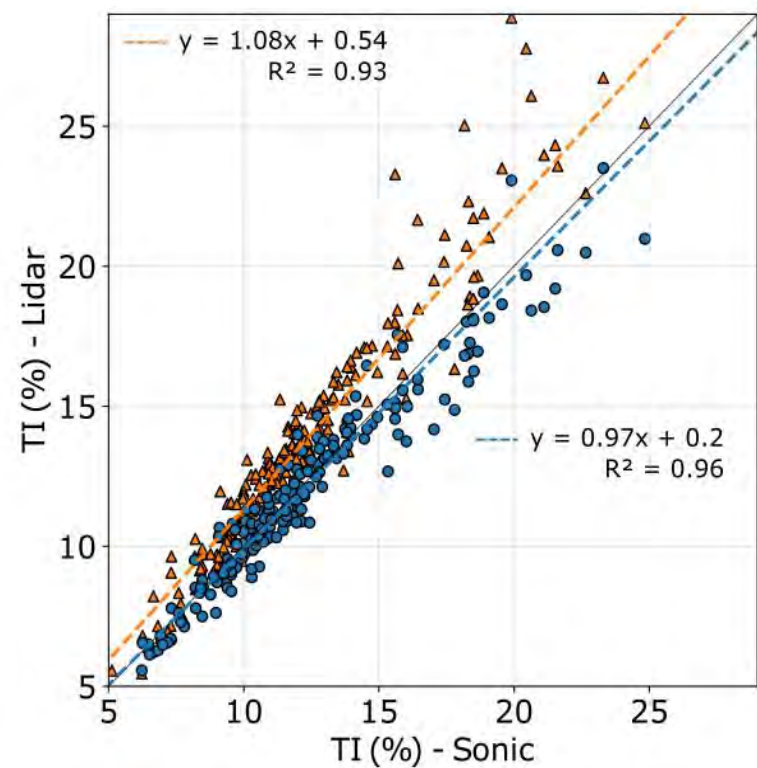


Standard Method vs. Variance Method

Wind aligned with opposite beams
(beam 1/beam 3 or beam 2/beam 4)

$$\sigma_{xy} = \sigma_{uv} \approx 0$$

$$\sigma_u^2 = \sigma_x^2 \cos^2 \vartheta + \sigma_y^2 \sin^2 \vartheta + \cancel{\sigma_{xy} \sin 2\vartheta}$$

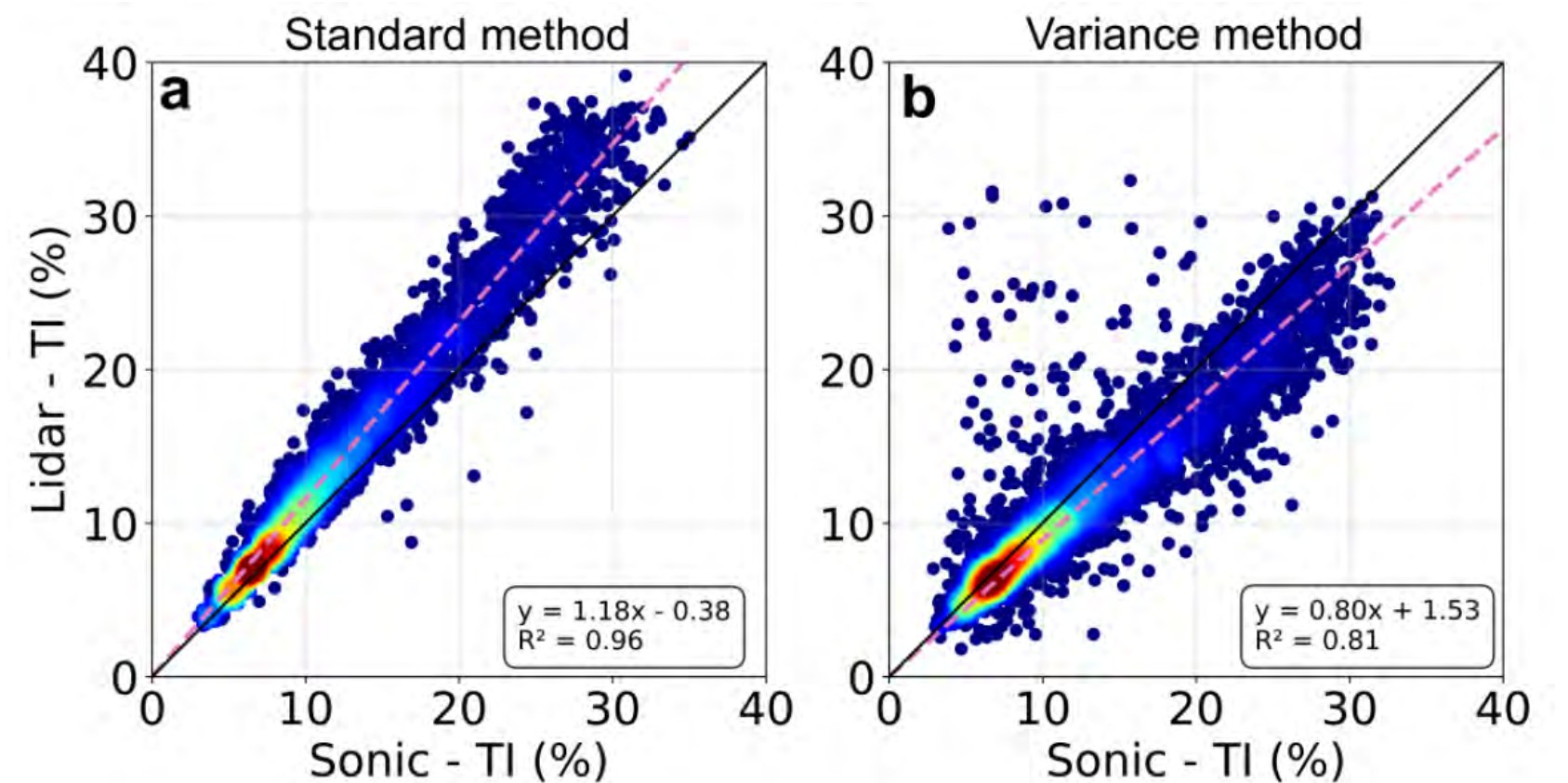


The variance method outperforms the standard method for each error statistics (MAE, RMSE, R²).

All wind directions

σ_{xy} not negligible but cannot be measured

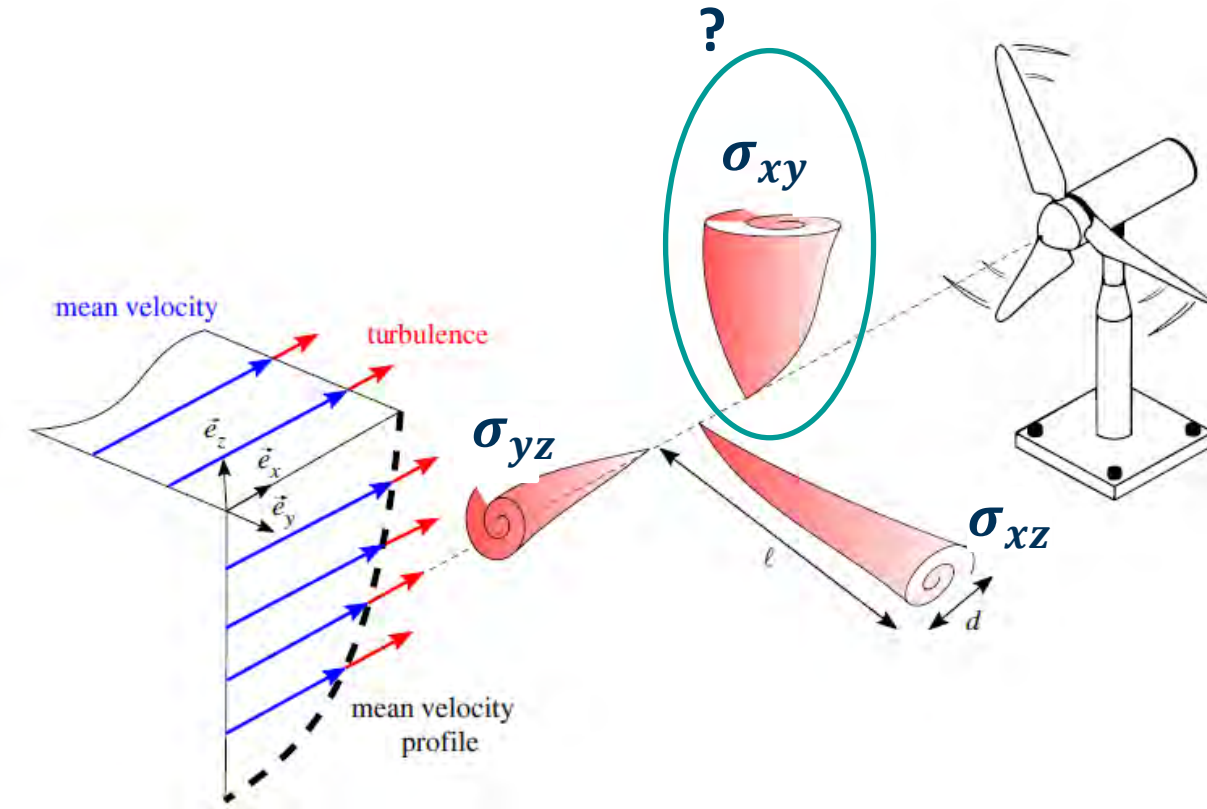
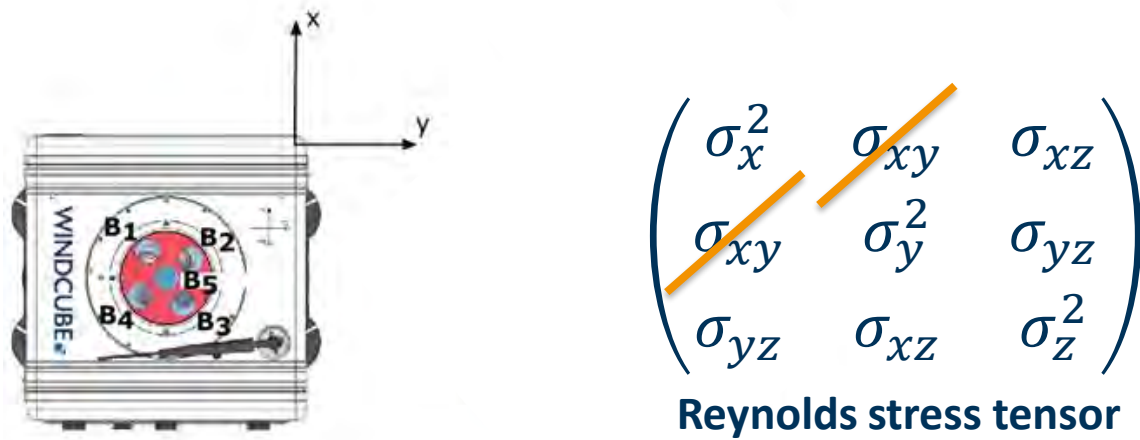
$$\sigma_u^2 = \sigma_x^2 \cos^2 \vartheta + \sigma_y^2 \sin^2 \vartheta + \sigma_{xy} \sin 2\vartheta$$



	TI (%) – Mean	MAE	RMSE	Bias	R ²
Sonic – Reference	12.9	-	-	-	-
Lidar – Standard method	14.9	2.05	2.87	1.92	0.96
Lidar – Variance method	11.7	1.87	2.70	-1.25	0.81

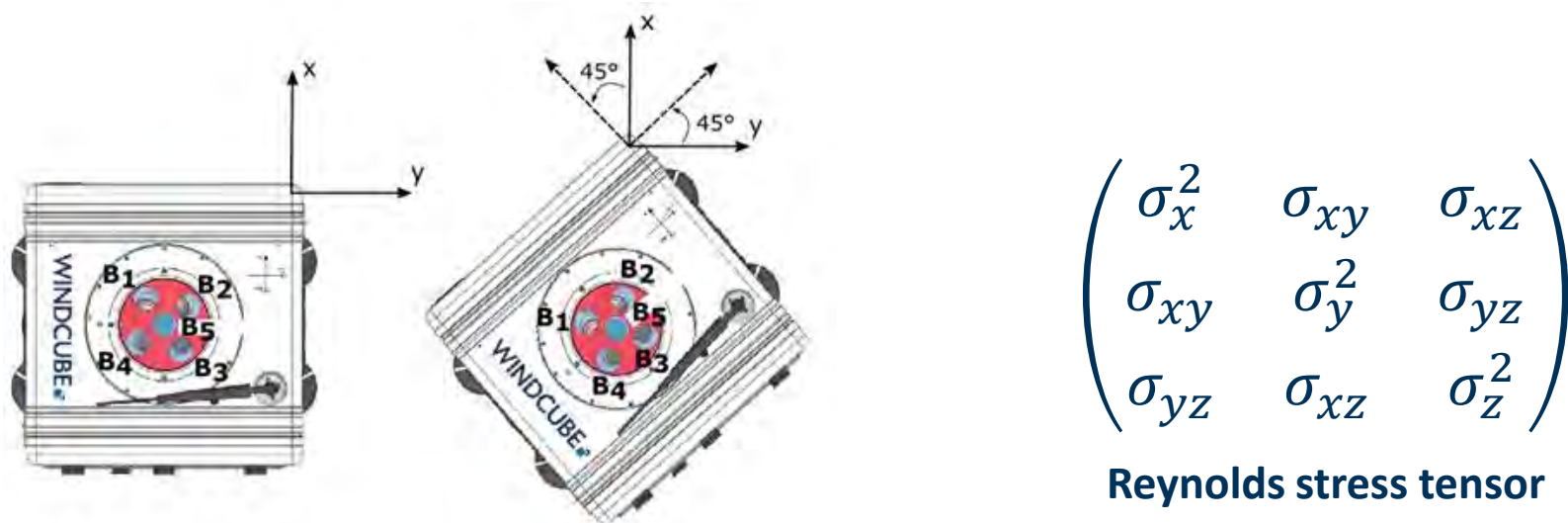
Variance Method – What's next?

- POWSEIDOM project (Oct. 2021 – April 2024)



- NEMO project (Nov. 2023 – May 2026) – Ongoing work

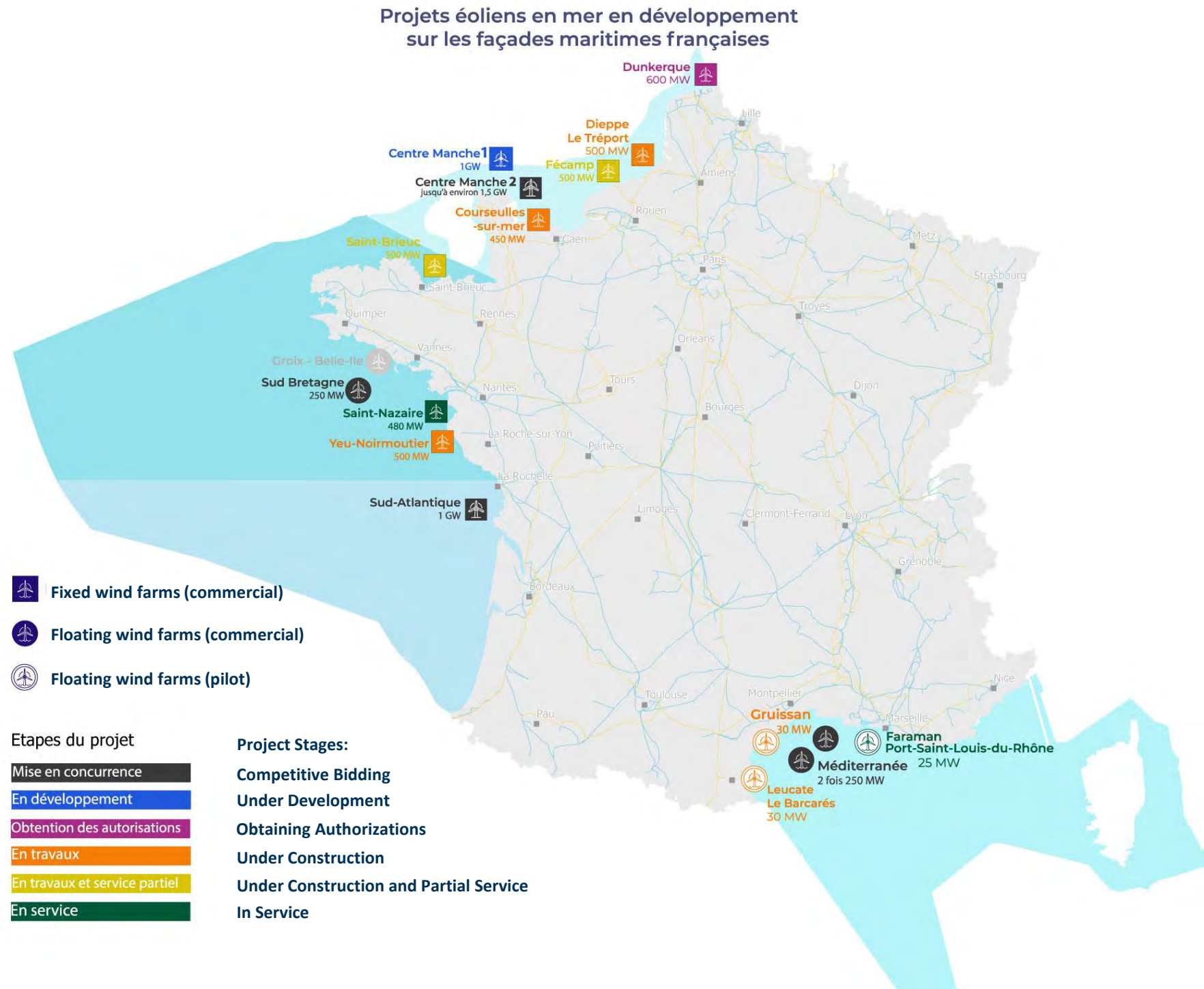
Coupling two lidar profiler to resolve the full Reynolds Stress Tensor :
TI computation for all wind directions.



Two coupled-lidar profilers installed on the Fécamp met. mast

Optimizing Sparse Sampling for Offshore Wind Resource Assessment in the Mediterranean Sea

Gaussian Mixture Models for the Optimal Sparse Sampling of Offshore Wind Resource



French Objectives :

- 15 GW by 2035
- 45 GW by 2050

45 GW spatial distribution :

- Channel & North Sea : 7 – 11GW
- North Atlantic : 6 – 9.5 GW
- South Atlantic : 2.5 – 5.5 GW
- Mediterranean Sea : 3 – 4.5 GW

Site characterization

- How many sensors are needed to capture most of the information required for offshore wind resource assessment?
- Where should these sensors be installed?

Wind Energ. Sci., 8, 771–786, 2023
<https://doi.org/10.5194/wes-8-771-2023>
 © Author(s) 2023. This work is distributed under the Creative Commons Attribution 4.0 License.



Gaussian mixture models for the optimal sparse sampling of offshore wind resource

Robin Marcille^{1,2}, Maxime Thiébaud¹, Pierre Tandeo², and Jean-François Filipot¹

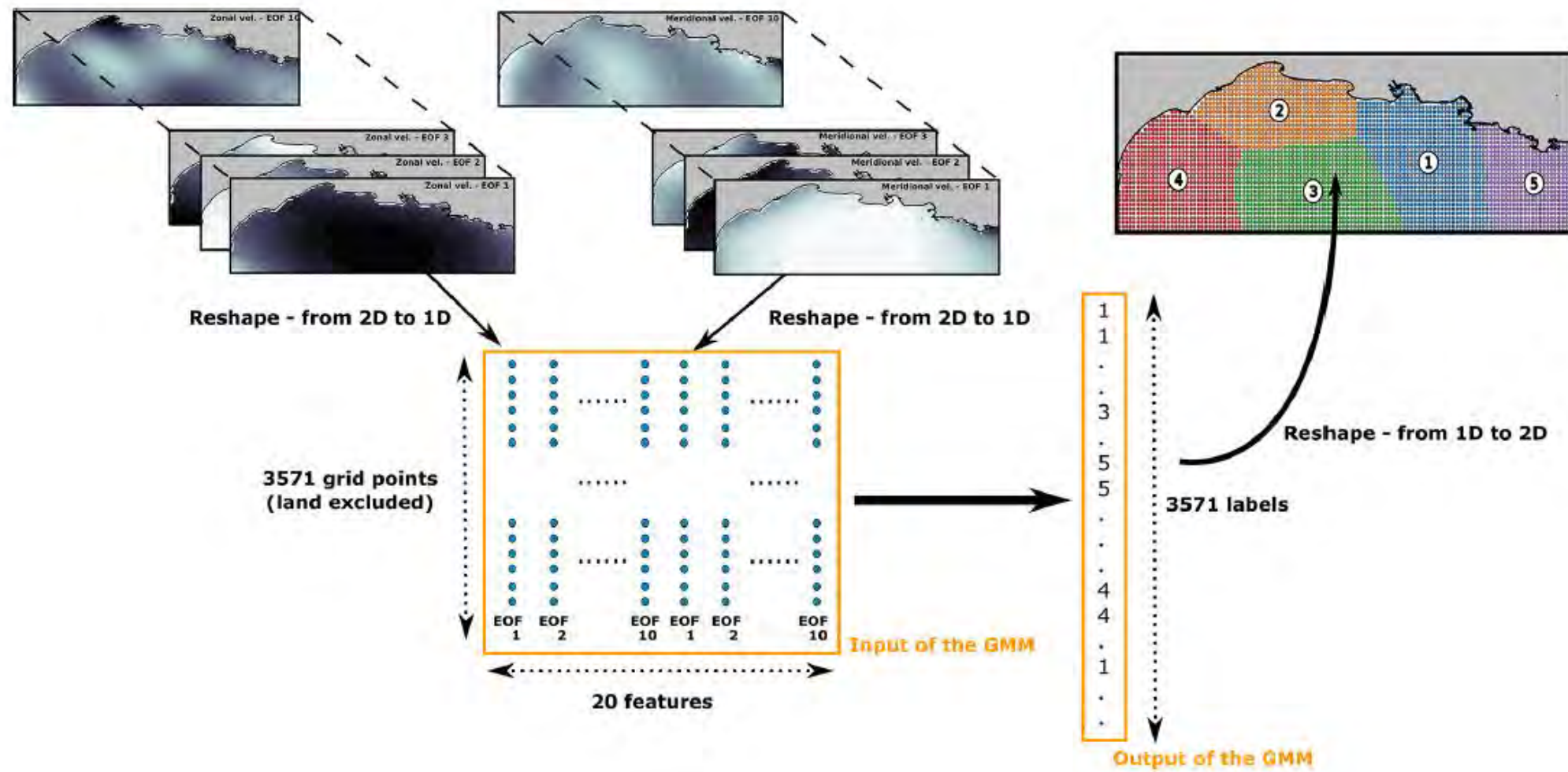
¹France Énergies Marines, Technopôle Brest-Iroise, 525 Avenue Alexis de Rochon, 29280 Plouzané, France

²IMT Atlantique, Lab-STICC, UMR CNRS 6285, 29238 Plouzané, France

Correspondence: Robin Marcille (robin.marcille@france-energies-marines.org)

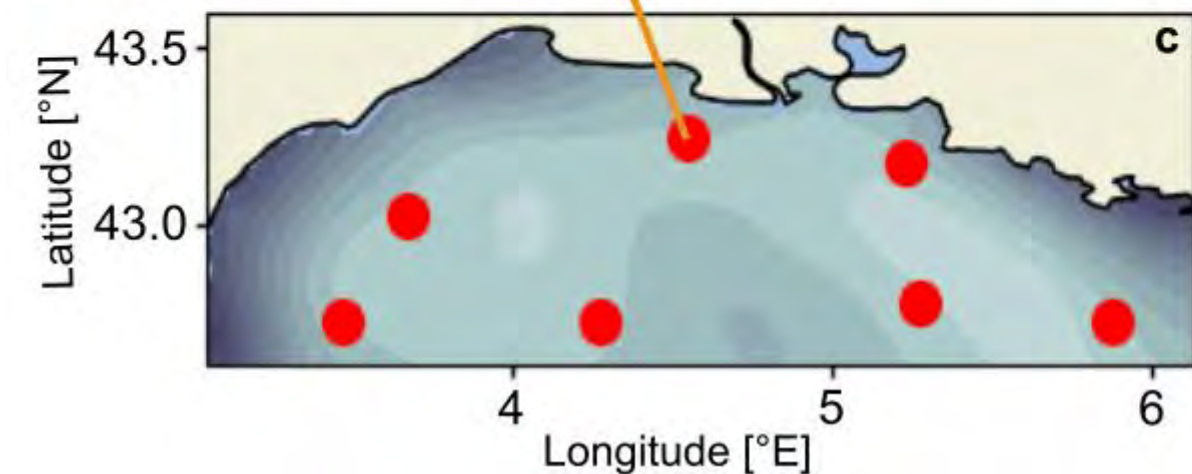
Received: 13 May 2022 – Discussion started: 2 June 2022
 Revised: 15 March 2023 – Accepted: 15 April 2023 – Published: 17 May 2023

The methodology is now employed by the Public Entity responsible for selecting the most suitable site for floating lidar profiler deployment during the site characterization stage.



Sensor no.	Lat (°N); Lon(°E)
1	42.775; 5.275
2	43.25; 4.55
3	42.725; 4.275
4	42.725; 3.475
5	43.175; 5.225
6	43.025; 3.675
7	42.725; 5.875

Le Planier Island



Deploying a Wind Lidar Profiler on Le Planier Island, Mediterranean Sea

Permanent Installation of a Certified Wind Lidar Profiler

- **Certified WindCube v2.1**, sampling **four times faster** than the standard commercial configuration;
- **Deployed in December 2022** and **still operational**;
- **Measurement altitudes**: Ranging from **60 to 220 meters** above sea level.

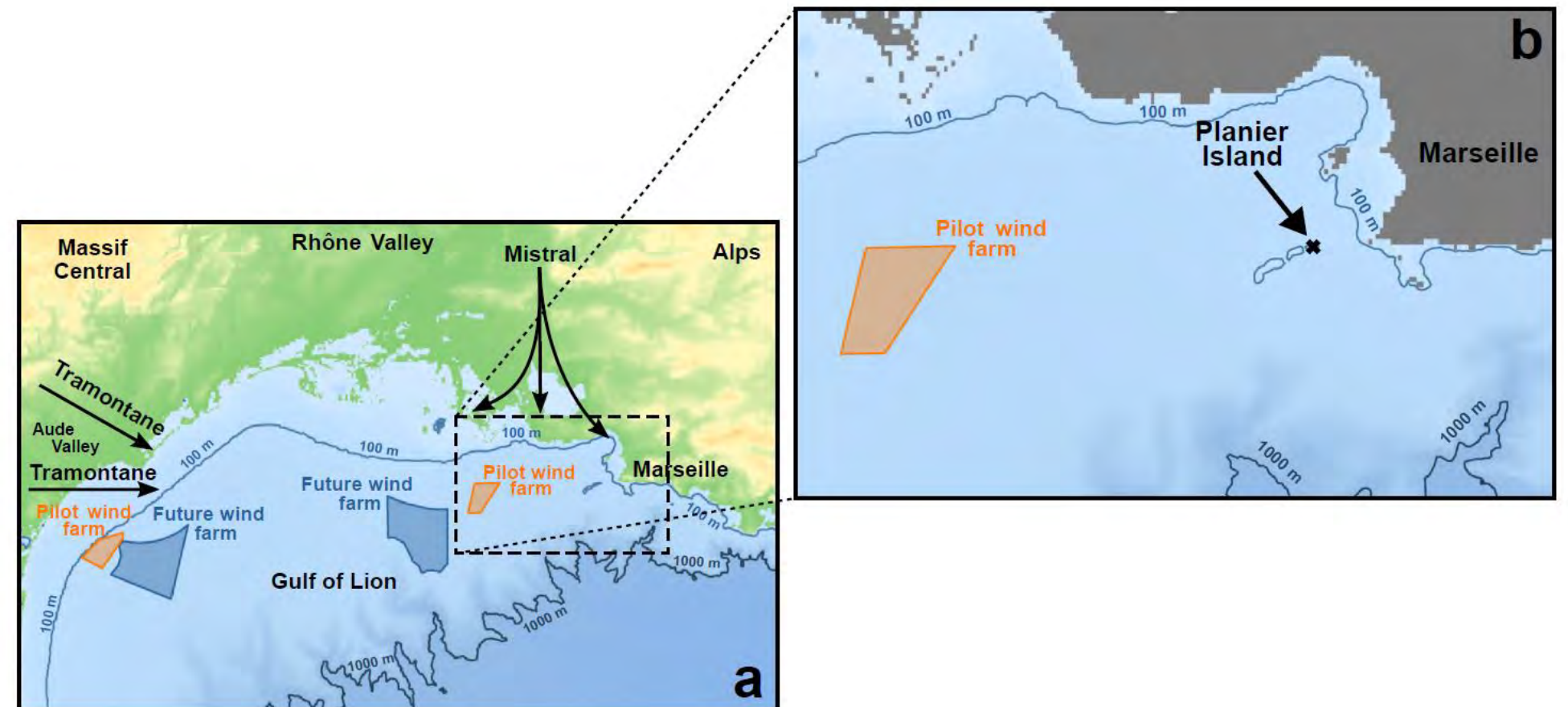


WLS7-1447

Independent performance verification at the DNV Remote Sensing Test Site in Janneby

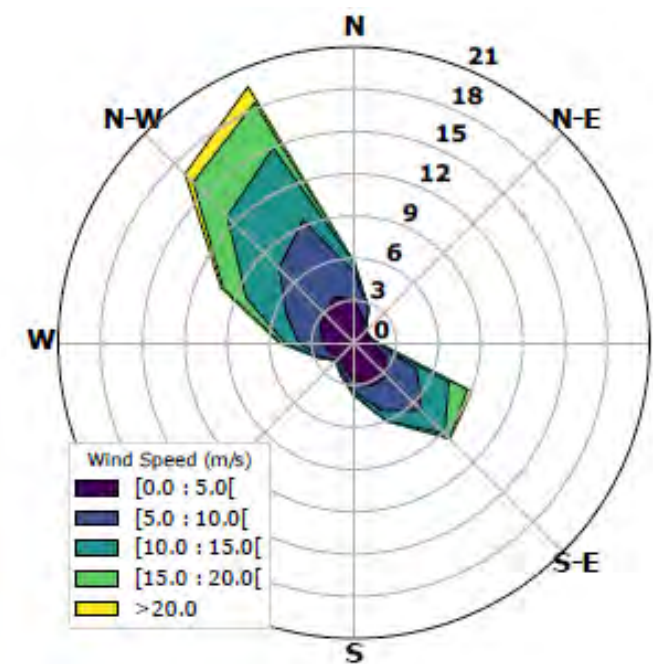
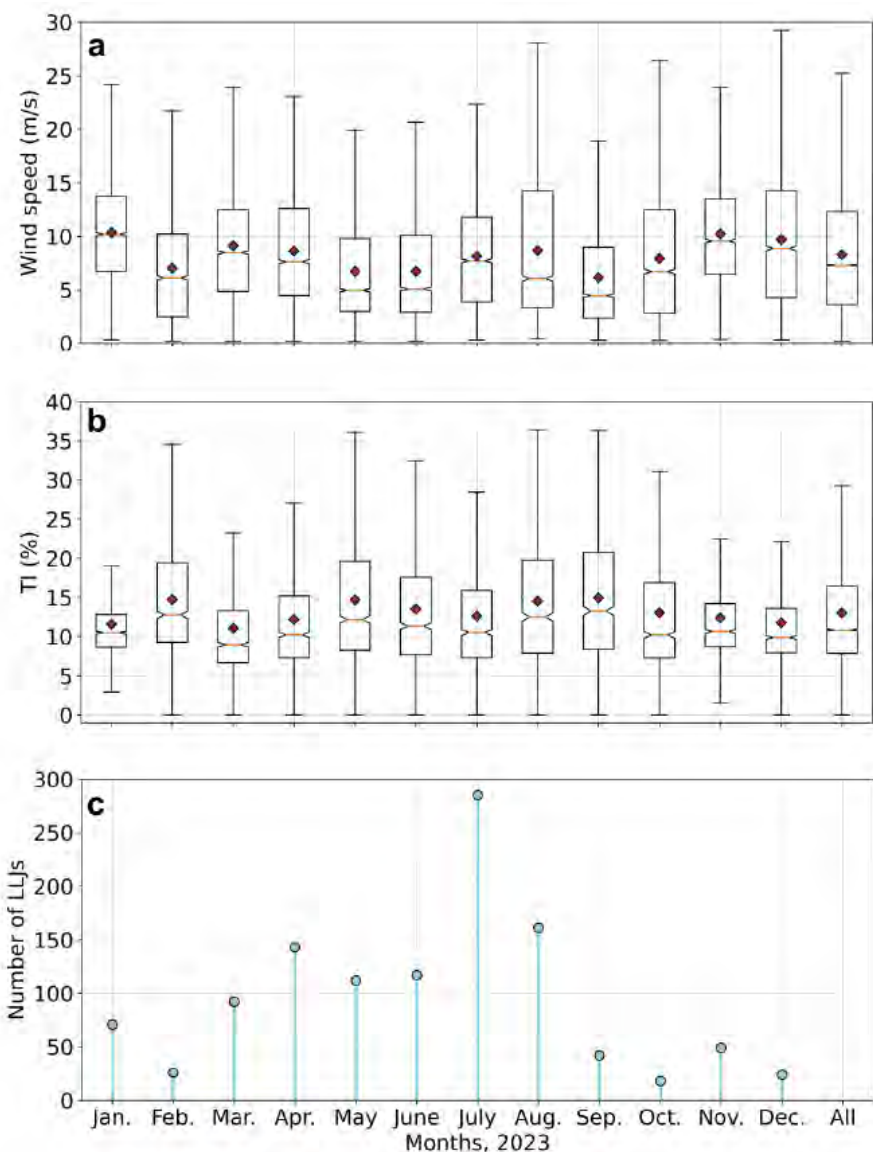
France Energies Marines

Report No.: 10318555-A-1-A, Rev. A
Date: 2022-05-25

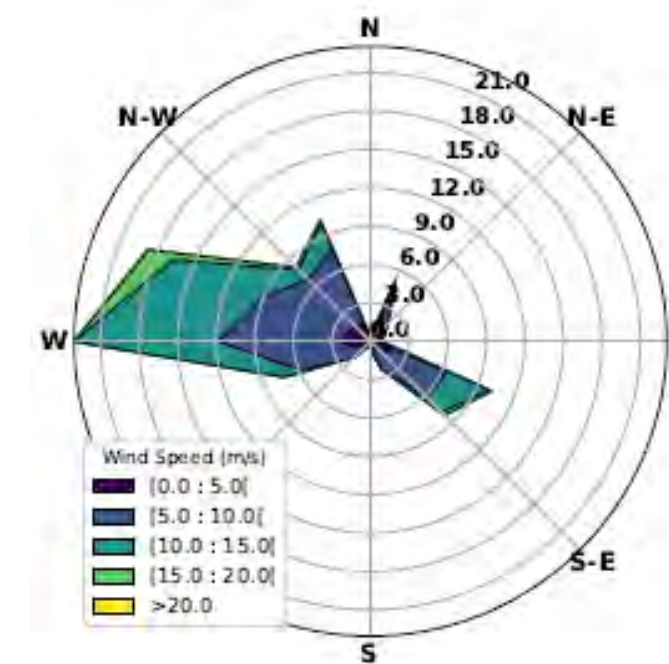


Characterization of the offshore wind dynamics for wind energy production in the Gulf of Lion

- Wind direction and veer
- Wind speed
- Wind speed profile and wind shear exponent
- Low-level jet
- Turbulence intensity (from both the standard and variance method)



Wind distribution patterns at 140 m above the sea level for the one-year dataset.



Wind direction and magnitude associated with the 1140 LLJs events detected over the one-year dataset.

Wind Energy and Engineering Research 1 (2024) 100002



Contents lists available at [ScienceDirect](https://www.sciencedirect.com)

Wind Energy and Engineering Research

journal homepage: www.elsevier.com/locate/weer



Characterization of the offshore wind dynamics for wind energy production in the Gulf of Lion, Western Mediterranean Sea

Maxime Thiébaud^{a,*}, Linta Vonta^a, Cristina Benzo^b, Florent Guinot^a

^a France Énergies Marines, Technopôle Brest-Iroise, 525 Avenue Alexis de Rochon, Plouzané 29280, France

^b Vaisala France SAS, 6A, rue René Razel, Tech Park, CS 70001, Saclay Cedex 91400, France



For each altitude of measurement, one-year (2023) time series of mean:

- **Wind Speed** (10-minute and 30-minute averages)
- **Wind Direction** (10-minute and 30-minute averages)

30-minute Average:

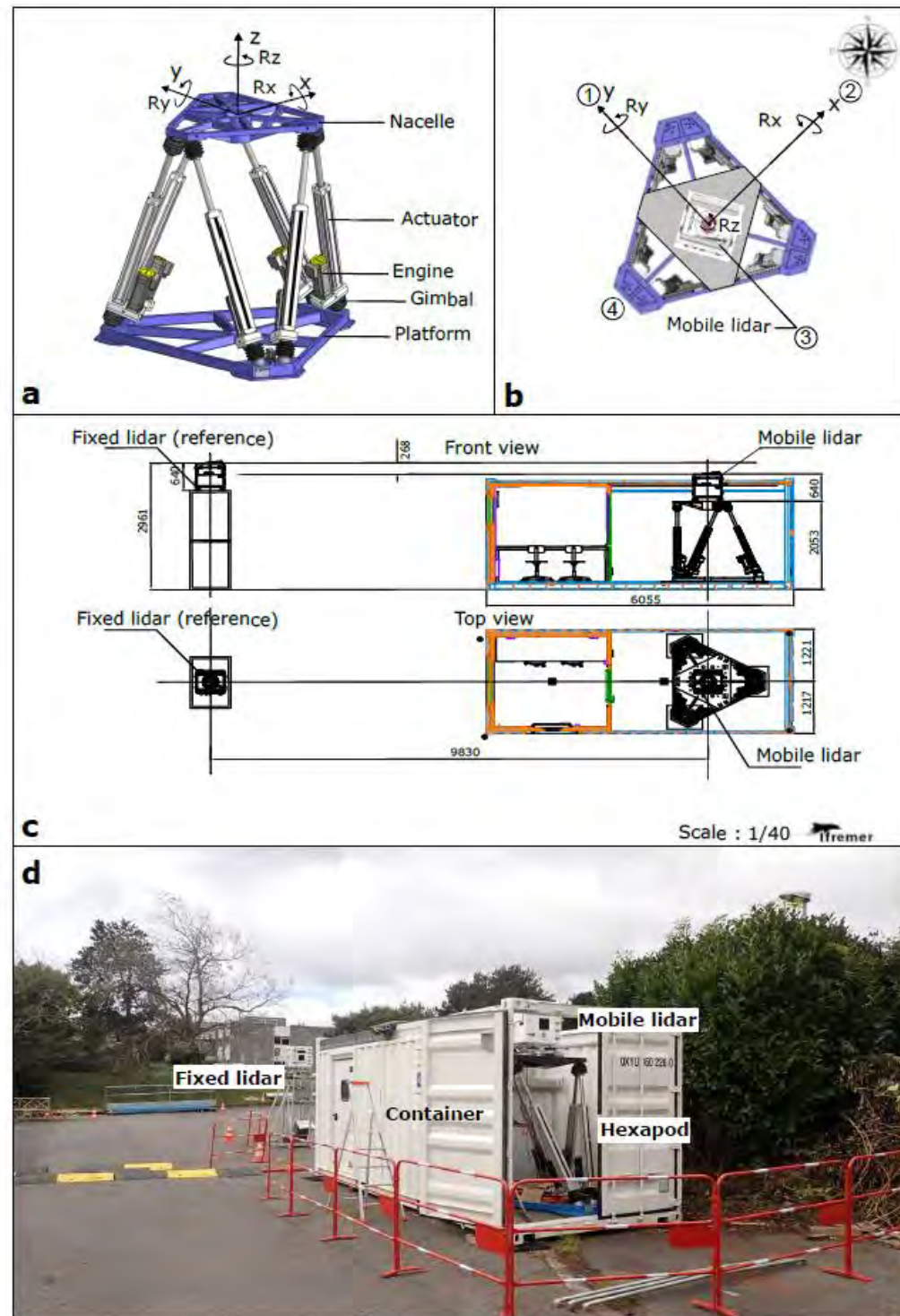
- Along-wind, cross-wind, and vertical wind **Turbulence Intensity (TI)** (calculated using both standard and variance methods)
- Along-wind, cross-wind, and vertical wind **Turbulent Kinetic Energy (TKE)** (calculated using both standard and variance methods)
- **Vertical Integral Length Scale** (directly measured by beam 5)
- **Dissipation Rate** (directly measured by beam 5)

```
TI_along_wind_standard_method.csv
1 time -> 60.m -> 80.m -> 100.m -> 120.m -> 140.m -> 160.m -> 180.m -> 200.m -> 220.m -> 240.m
2 2023-01-01 00:15 -> 10.428794295297338 -> 9.661655673185729 -> 8.832811677906008 -> 8.105457301754225 -> 7.513688133406992 -> 7.2485755108458925 -> 7.825832371042134 -> 8.86556643638529 -> 10.321249015220546 -> 11.288319746716224
3 2023-01-01 00:45 -> 7.71865174298311 -> 6.962598722880084 -> 6.6219964722901645 -> 6.430468234801603 -> 6.27622172218832 -> 6.46310478938597 -> 7.174253211303933 -> 8.253033416720543 -> 9.038182013956645 -> 10.55732191473649
4 2023-01-01 01:15 -> 7.9722239765168315 -> 6.2235908957496004 -> 5.687657676399476 -> 5.359607377637643 -> 4.992736185307604 -> 4.674051752735997 -> 4.44038574079425 -> 4.496044244364838 -> 4.880482275565942 -> 5.117528827277281
5 2023-01-01 01:45 -> 8.166507561662204 -> 5.5163139838585185 -> 4.995685155353584 -> 4.348341293736432 -> 3.588271840397523 -> 3.0717203254750047 -> 2.807428316700559 -> 2.7841744080365003 -> 2.9204822861237263 -> 3.2837941112859386
6 2023-01-01 02:15 -> 8.802355529873877 -> 6.104890662905422 -> 5.667382251691942 -> 5.0107755648083545 -> 4.588492121386013 -> 4.419365140314349 -> 4.3278388128045915 -> 4.155499855835771 -> 3.923011470160123 -> 3.7238924032159364
7 2023-01-01 02:45 -> 8.283608463265429 -> 6.661236254126701 -> 6.646572898706626 -> 6.492939451646997 -> 6.428968981794019 -> 6.256762486948056 -> 6.107257649849031 -> 6.087761685751706 -> 5.91821023704429 -> 5.6013592409510755
8 2023-01-01 03:15 -> 7.384145538600441 -> 5.364419035428955 -> 4.932916529290367 -> 4.7014000635556155 -> 4.615677357496106 -> 4.587719507745943 -> 4.350723794881981 -> 4.3562374481734185 -> 4.203589138820367 -> 4.048205785576003
9 2023-01-01 03:45 -> 8.690436251067284 -> 5.766878741013332 -> 5.067298765876668 -> 4.360351346380977 -> 3.895699170762347 -> 3.664207982571706 -> 3.4263648853790962 -> 3.1749447692862107 -> 3.1142954300227945 -> 3.1585248953595007
10 2023-01-01 04:15 -> 8.125800550050034 -> 5.5688077094481 -> 4.833862857905917 -> 4.300566274925205 -> 4.013816871325474 -> 3.706520409962678 -> 3.5523806675141865 -> 3.537940092393315 -> 3.640114087363829 -> 3.833743348686892
```

Example of the architecture of a csv file.

Such a dataset can be derived for any period upon request.

Developing a Preliminary Motion-Compensation Algorithm for Floating Lidar Turbulence Measurement



Article

Experimental Evaluation of the Motion-Induced Effects for Turbulent Fluctuations Measurement on Floating Lidar Systems

Maxime Thiébaud ^{1,*}, Nicolas Thebault ¹, Marc Le Boulluec ², Guillaume Damblans ¹, Christophe Maisondieu ², Cristina Benzo ³ and Florent Guinot ¹

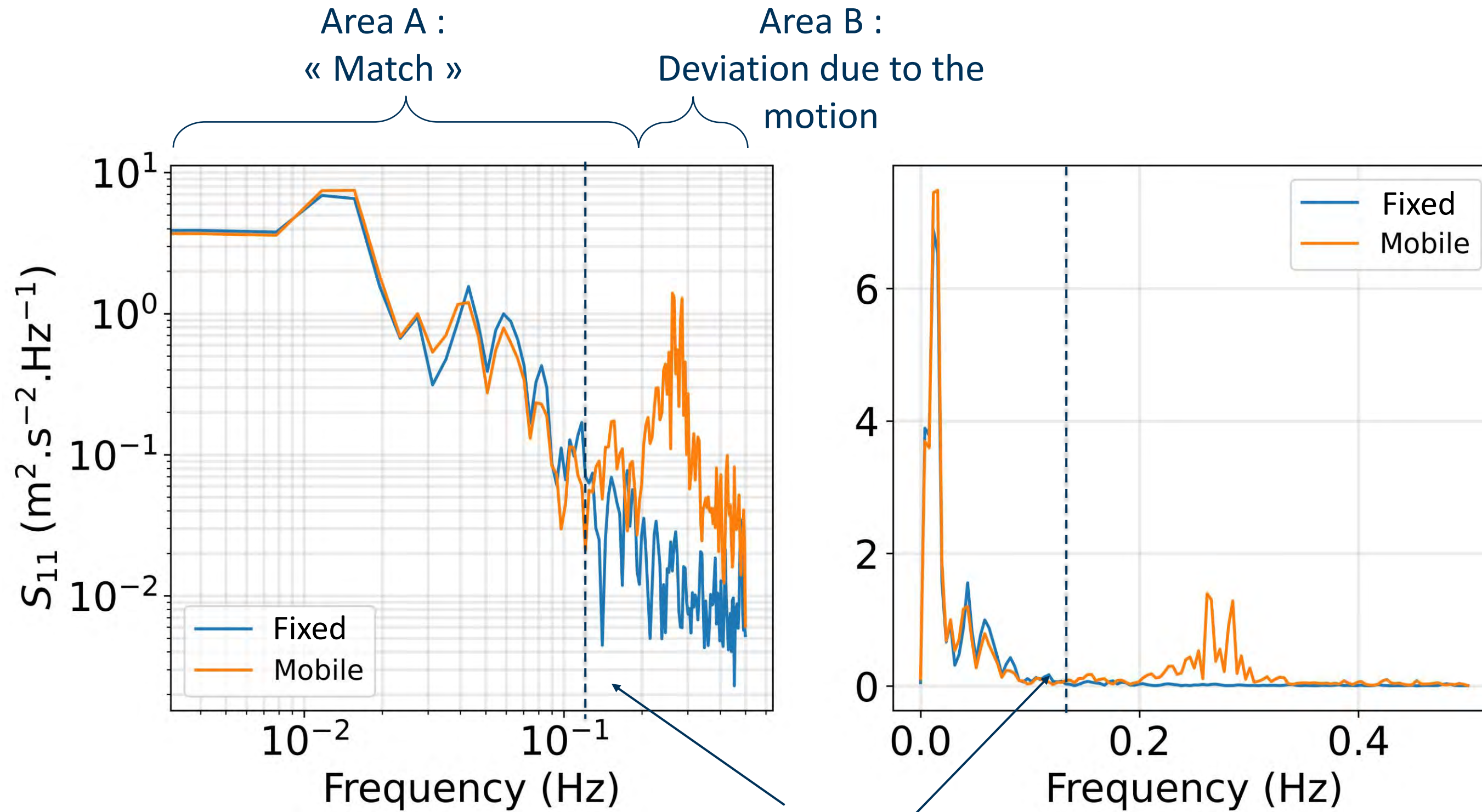
- 15 cycles of 3-hour long collected between October 6th, November 9th 2022.
- 1 cycle is composed of 12 sequences (regular and irregular motions).

Regular motions

Sequences (30-min)	Ry	Rx	Rz
S1	T = 4s; A = 5°	NA	NA
S2	T = 4s; A = 15°	NA	NA
S3	T = 6s; A = 5°	NA	NA
S4	T = 6s; A = 15°	NA	NA
S5	T = 8s; A = 5°	NA	NA
S6	T = 8s; A = 15°	NA	NA
S7	T = 6s; A = 5°	T = 6s; A = 5°	NA
S8	T = 6s; A = 5°	NA	T = 6s; A = 5°
S9	T = 6s; A = 5°	T = 6s; A = 5°	T = 6s; A = 5°

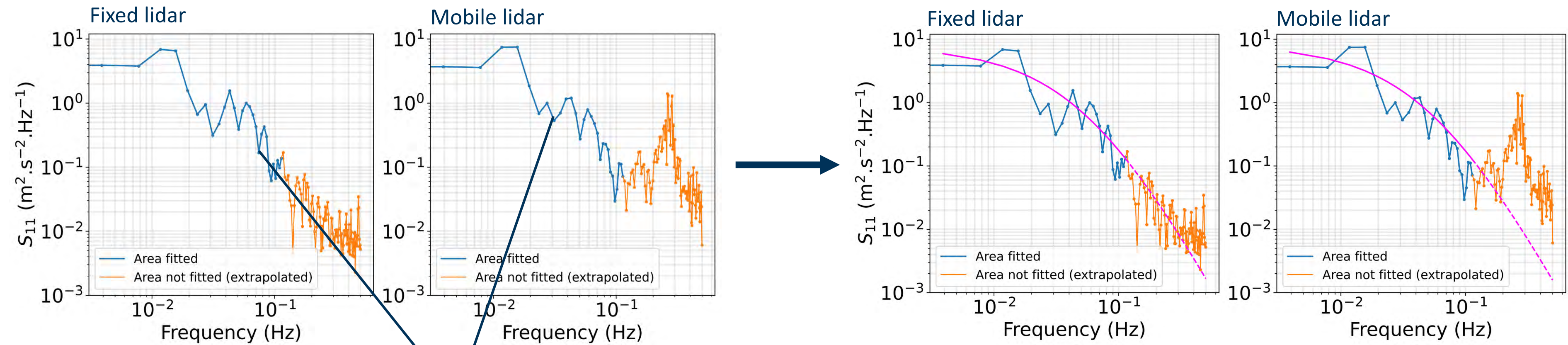
Irregular motions

Sequences (30-min)	Ry	Rx	Rz
S10	T = 2-20s	NA	NA
S11	Hs = 0.7m, Tp=4s, 225°		NA
S12	Hs = 0.7m, Tp = 4s, 225°		Hs = 2m, Tp = 6s, 180°

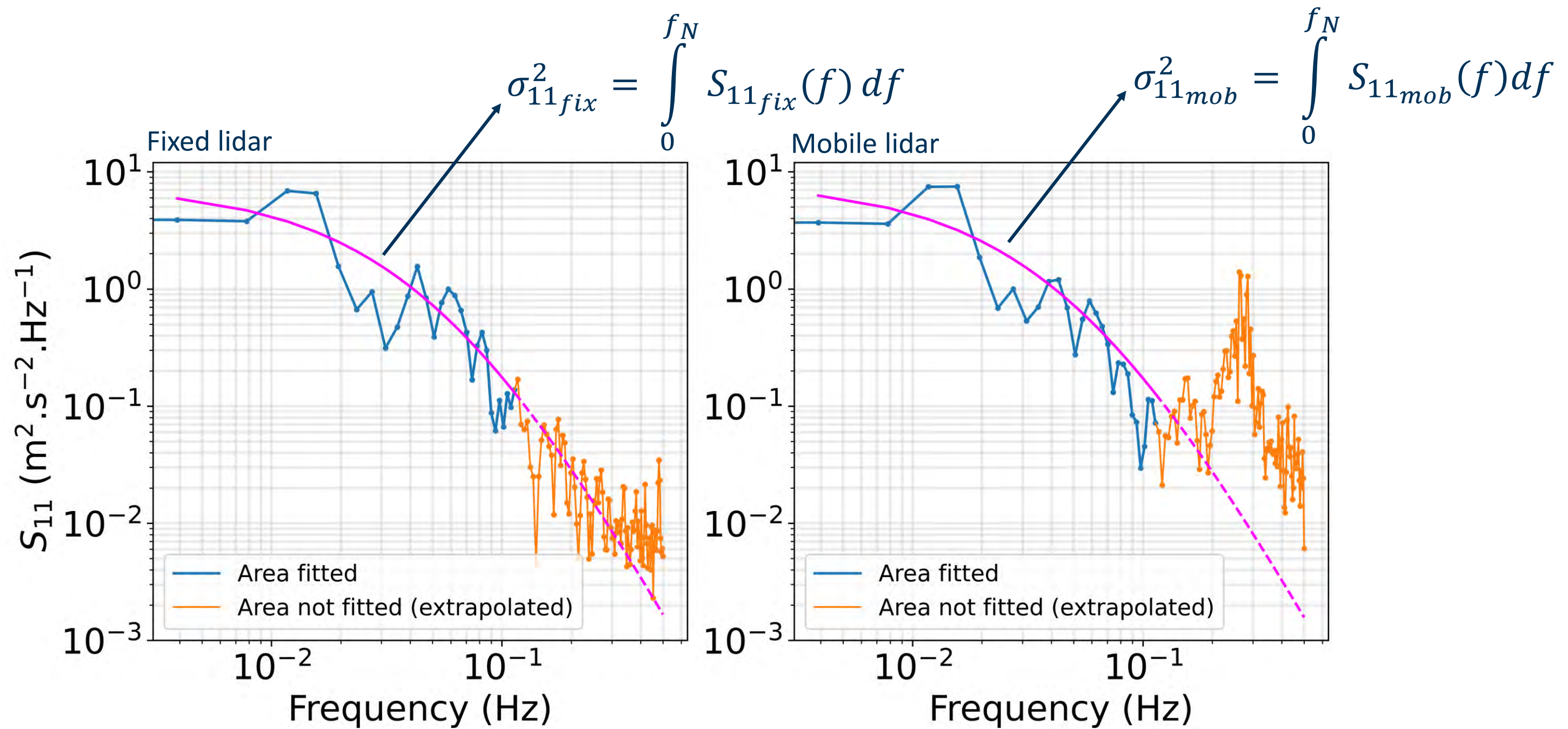


An algorithm finds automatically the cutting frequency for each spectrum derived from the mobile lidar

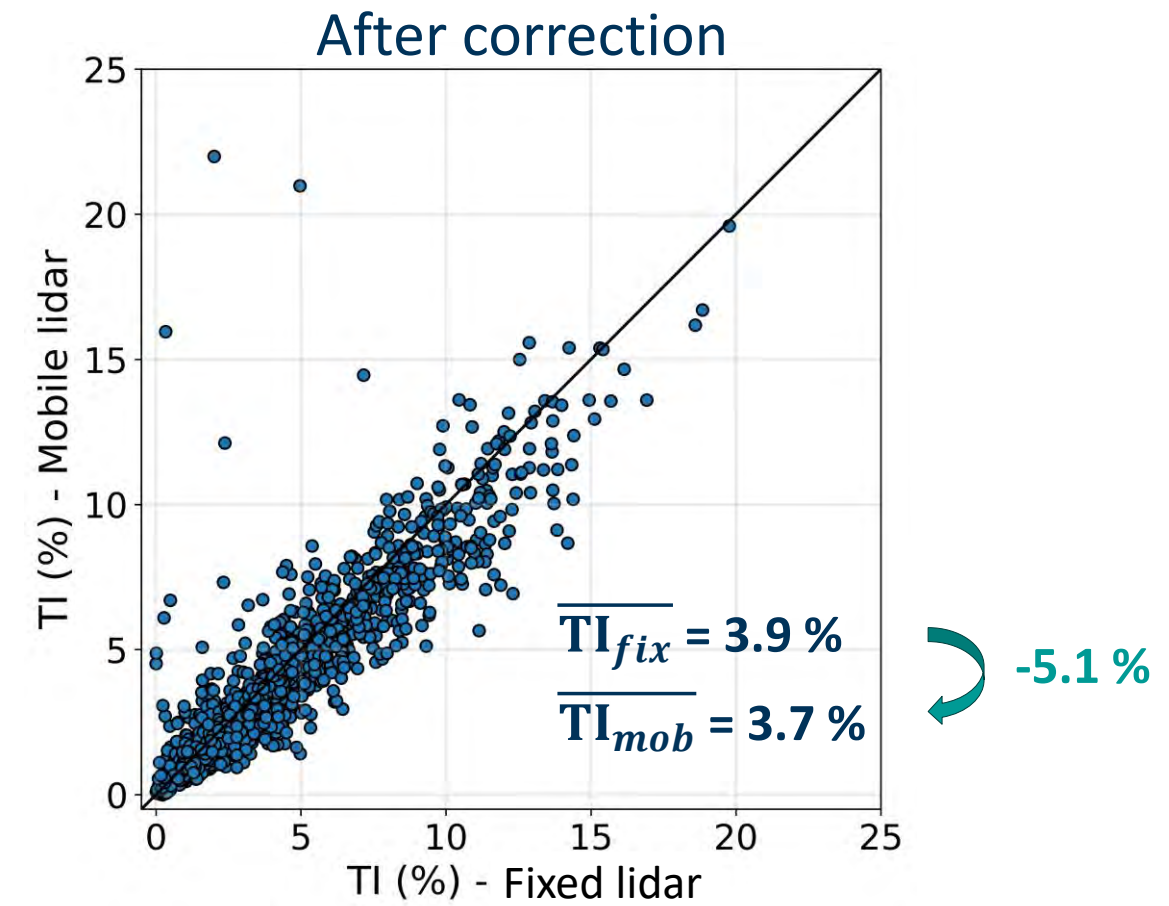
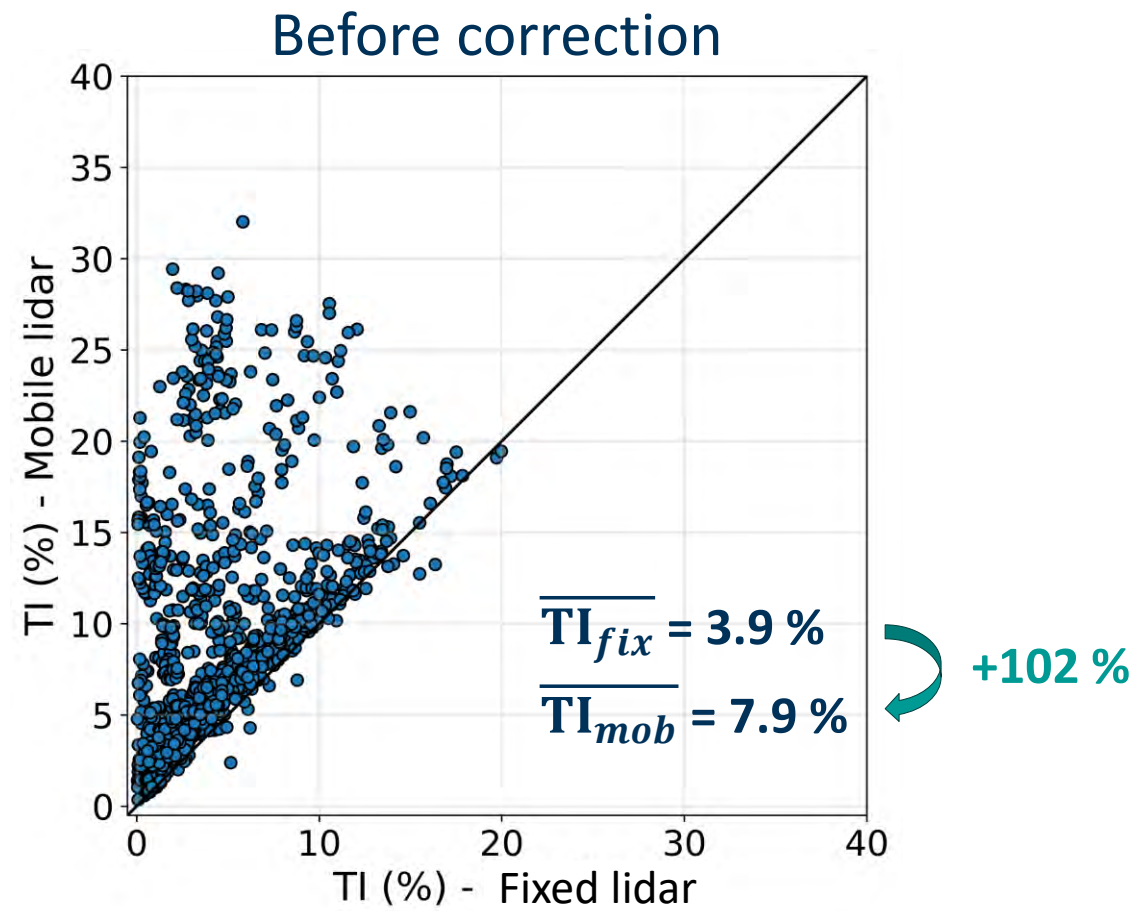
$$\text{Fitting function : } S = \frac{a}{(1 + nf)^\beta}$$



Fitting performed on 30 points (23% of the length of each spectrum)



Preliminary Motion-Compensation Algorithm



	Before correction	After correction
TI - RMSE (%)	6.8	1.7
TI - MAE (%)	4.0	0.8
TI - Bias (%)	3.95	-0.2

Thank you for your attention!

